

First Observation of the Reaction

$$\gamma\gamma \rightarrow \pi_2 \rightarrow \pi^{\circ}\pi^{\circ}\pi^{\circ}$$

The Crystal Ball Collaboration

D. Antreasyan⁹, H.W. Bartels⁵, D. Besset¹¹, Ch. Bieler⁸, J.K. Bienlein⁵, A. Bizzeti⁷,
 E.D. Bloom¹², I. Brock³, K. Brockmüller⁵, R. Cabenda¹¹, A. Cartacci⁷, M. Cavalli-Sforza²,
 R. Clare¹², A. Compagnucci⁷, G. Conforto⁷, S. Cooper^{12,a}, R. Cowan¹¹, D. Coyne²,
 A. Engler³, K. Fairfield¹², G. Folger⁶, A. Fridman^{12,b}, J. Gaiser¹², D. Gelphman¹²,
 G. Glaser⁶, G. Godfrey¹², K. Graaf⁸, F.H. Heimlich⁷, F.H. Heinsius⁸, R. Hofstadter¹²,
 J. Irion⁹, Z. Jakubowski⁵, H. Janssen¹⁰, K. Karch⁵, S. Keh¹³, T. Kiel⁸, H. Kilian¹³,
 I. Kirkbride¹², T. Kloiber⁵, M. Kobel⁶, W. Koch⁵, A.C. König¹⁰, K. Königsmann^{13,c},
 R.W. Kraemer³, S. Krüger⁸, G. Landi⁷, R. Lee¹², S. Leffer¹², R. Lekebusch⁸, A.M. Litke¹²,
 W. Lockman¹², S. Lowe¹², B. Lurz⁶, D. Marlow³, H. Marsiske^{5,12}, W. Maschmann⁵,
 P. McBride⁹, F. Messing³, W.J. Metzger¹⁰, H. Meyer⁵, B. Monteleoni⁷, B. Muryn^{4,d},
 R. Nernst⁸, B. Niczyporuk¹², G. Nowak⁴, C. Peck¹, P.G. Pelfer⁷, B. Pollock¹², F.C. Porter¹,
 D. Prindle³, P. Ratoff¹, M. Reidenbach¹⁰, B. Renger³, C. Rippich³, M. Scheer¹³,
 P. Schmitt¹³, J. Schotanus¹⁰, J. Schütte⁶, A. Schwarz¹², D. Sievers⁸, T. Skwarnicki⁵,
 V. Stock⁸, K. Strauch⁹, U. Strohbusch⁸, J. Tompkins¹², H.J. Trost⁵, B. van Uiter¹²,
 R.T. Van de Walle¹⁰, H. Vogel³, A. Voigt⁵, U. Volland⁶, K. Wachs⁵, K. Wacker¹²,
 W. Walk¹⁰, H. Wegener⁶, D. A. Williams^{9,2}, P. Zschorsch⁵

¹ California Institute of Technology^e, Pasadena, CA 91125, USA

² University of California at Santa Cruz^f, Santa Cruz, CA 95064, USA

³ Carnegie-Mellon University^g, Pittsburgh, PA 15213, USA

⁴ Cracow Institute of Nuclear Physics, PL-30055 Cracow, Poland

⁵ Deutsches Elektronen Synchrotron DESY, D-2000 Hamburg, Germany

⁶ Universität Erlangen-Nürnberg^h, D-8520 Erlangen, Germany

⁷ INFN and University of Firenze, I-50125 Firenze, Italy

⁸ Universität Hamburg, I. Institut für Experimentalphysikⁱ, D-2000 Hamburg, Germany

⁹ Harvard University^j, Cambridge, MA 02138, USA

¹⁰ University of Nijmegen and NIKHEF^k, NL-6525 ED Nijmegen, The Netherlands

¹¹ Princeton University^l, Princeton, NJ 08544, USA

¹² Department of Physics^m, HEPL, and Stanford Linear Accelerator Centerⁿ,

Stanford University, Stanford, CA 94309, USA

¹³ Universität Würzburg^o, D-8700 Würzburg, Germany

ABSTRACT

The Crystal Ball detector has been used at the DORIS II storage ring at DESY to study the reaction $\gamma\gamma \rightarrow \pi^+\pi^-\pi^0$ in the $\pi^+\pi^-\pi^0$ invariant mass range from 850 MeV/c² to 2600 MeV/c². An enhancement around 1750 MeV/c² is attributed to the $\pi_2(1670)$ resonance. The observed $\pi^+\pi^0$ invariant mass distribution and the π^0 angular distributions are consistent with those expected for the decay chain $\pi_2 \rightarrow \pi^0 f_2(1270) \rightarrow \pi^0 \pi^0 \pi^0$. From our measurements we find the following resonance parameters: two photon partial width $\Gamma_{\pi_2}^{\gamma\gamma} = (1.45 \pm 0.23 \pm 0.28)$ keV, mass $M(\pi_2) = (1742 \pm 31 \pm 49)$ MeV/c² and total width $\Gamma_{\pi_2}^{tot} = (236 \pm 49 \pm 36)$ MeV.

(Submitted to Zeitschrift für Physik C)

-
- a) Present Address: Max-Planck-Institut für Physik, D-8000 München 40, Germany
b) Permanent Address: DPHPE, Centre d'Etudes Nucléaires de Saclay, F-91191 Gif sur Yvette, France
c) Permanent Address: CERN, CH-1211 Genève 23, Switzerland
d) Permanent Address: Institute of Physics and Nuclear Techniques, AGH, PL-30055 Cracow, Poland
e) Supported by the U.S. Department of Energy, contract No. DE-AC03-81ER40050 and by the National Science Foundation, grant No. PHY75-22980
f) Supported by the National Science Foundation, grant No. PHY85-12145
g) Supported by the U.S. Department of Energy, contract No. DE-AC02-76ER03066
h) Supported by the German Bundesministerium für Forschung und Technologie, contract No. 054 ER 11P(5)
i) Supported by the German Bundesministerium für Forschung und Technologie, contract No. 054 HH 11P(7) and by the Deutsche Forschungsgemeinschaft
j) Supported by the U.S. Department of Energy, contract No. DE-AC02-76ER03064
k) Supported by FOM-NWO
l) Supported by the U.S. Department of Energy, contract No. DE-AC02-76ER03072 and by the National Science Foundation, grant No. PHY82-08761
m) Supported by the U.S. Department of Energy, contract No. DE-AC03-76SF00326 and by the National Science Foundation, grant No. PHY81-07396
n) Supported by the U.S. Department of Energy, contract No. DE-AC03-76SF00515
o) Supported by the German Bundesministerium für Forschung und Technologie, contract No. 054 WU 11P(1)

1 Introduction

In this paper the $\gamma\gamma$ production of the $\pi_2(1670)$ resonance and the measurement of its radiative width, mass and total width is reported. This resonant state has been known since 1965 and has been confirmed by several experiments [1]. The π_2 has $J^{PC} = 2^{-+}$ and is believed to belong to the nonet in which the quark and the antiquark spins are coupled to a singlet state having orbital angular momentum $L = 2$. Having positive C -parity and $J \neq 1$, it is accessible in quasi-real $\gamma\gamma$ scattering at e^+e^- storage rings.

The strength of the two-photon coupling is an important observable of any resonance. In the quark model it is proportional to $\langle e_q^2 \rangle_R^2$, where $\langle e_q^2 \rangle_R$ is the mean squared charge of the quark constituents q of the resonance R . This information can test our understanding of mesons and helps in the classification of new states.

In this analysis the neutral member of the π_2 isotriplet has been observed via its $\pi^0 f_2(1270)$ decay in the reaction chain

$$e^+e^- \rightarrow e^+e^- + \pi_2(1670) \left. \begin{array}{l} \hookrightarrow \pi^0 f_2(1270) \\ \hookrightarrow \pi^0\pi^0 \end{array} \right\} \rightarrow \pi^0\pi^0\pi^0 \rightarrow 6\gamma. \quad (1)$$

The measurement was performed at an average beam energy of 5 GeV using the Crystal Ball detector at the DORIS II e^+e^- storage ring. Preliminary results have been reported at the Shores conference on photon-photon collisions [2]. The CELLO Collaboration has observed the $\pi_2(1670)$ in the reaction chain $\gamma\gamma \rightarrow \pi_2 \rightarrow \pi^+\pi^-\pi^0$ [3].

The paper is organized as follows: in the next section the Crystal Ball detector is briefly described. The method of π^0 identification and the event selection are explained in sections 3 and 4. In section 5 the detection efficiency and Monte Carlo event simulation are discussed. The following three sections are devoted to background subtraction (section 6), angular distributions (section 7) and results on the π_2 resonance parameters (section 8). Finally, section 9 contains the conclusions.

2 Detector

The Crystal Ball detector is a non-magnetic calorimeter designed to measure precisely the energies and directions of electromagnetically showering particles. It is well suited to study two-photon collisions in which all the final state particles are photons. The main part of the detector is a spherical shell of 672 optically isolated NaI(Tl) crystals covering 93% of the total solid angle. A large geometrical acceptance is important for the detection of final states produced in two-photon reactions. Because of generally unequal initial state photon energies, the two-photon center-of-mass system is moving in the laboratory frame and the

final state particles are boosted along the beam direction. The energy resolution for photons is $\sigma_E/E = (2.7 \pm 0.2)\%/\sqrt{E(\text{GeV})}$. The photon direction θ with respect to the beam axis is determined, using the NaI calorimeter, with an accuracy of $\sigma_\theta = 1^\circ$ to 3° depending on the photon energy. To detect charged particles the central cavity of the Crystal Ball is equipped with a set of four cylindrical double layers of tube chambers. For the first 87 pb^{-1} of the full 257 pb^{-1} sample, only three double layers were installed. The azimuthal angle ϕ and the position of the hit along the z -direction (the initial e^+ direction of flight) are measured. A detailed description of the Crystal Ball detector has been given elsewhere [4].

3 Identification of neutral pions

In this experiment the final state leptons were not observed since they are predominantly scattered at very small angles. Hence the observed final state consists of six photons. Each of these photons is detected by its energy deposition in a region of adjacent crystals each having at least 10 MeV, called a “connected region”. In the case of well-separated photons one should detect six energy clusters for the $\pi^0\pi^0\pi^0$ final state. However, the energy of at least one of the three π^0 's is usually relatively large because of the high mass of the π_2 and the f_2 as well as the boost of the $\gamma\gamma$ system. The two photons originating from such a π^0 have a small opening angle. This results in overlapping energy deposits forming just one energy cluster in the detector. We call this a “merged π^0 ”, as opposed to an “unmerged π^0 ”, where the two decay photons form two isolated clusters. For the granularity of the Crystal Ball detector this merging starts to occur for π^0 energies of about 500 MeV. Hence we search for events with five energy clusters: four from well separated photons from the decay of two π^0 's, and one cluster from the two unresolved photon showers from the remaining fast π^0 .

Unmerged π^0 's are reconstructed from pairs of separated photon candidates. A connected region is a separated photon candidate if its lateral energy distribution is consistent with that expected for an electromagnetically showering particle. The photon energy and direction are determined from the crystal with the highest energy in the connected region and its twelve nearest neighbors. Small corrections to the energy are applied as described below.

Connected regions with total energy greater than 500 MeV are candidates for merged π^0 's. Their identification is based on an algorithm [5] which evaluates the transverse shower pattern. The energy E and direction \vec{c} of the merged π^0 candidate are calculated by $E = \sum_i E_i$ and $\vec{c} = \sum_i E_i \vec{n}_i / E$, respectively, where E_i is the energy detected in the i^{th} crystal, \vec{n}_i is the unit vector pointing to its center, and the sums run over all crystals in the connected region. This energy is then corrected for longitudinal and lateral shower leakage (see below). From the second moment of the lateral energy distribution, defined as $s \equiv \sum_i (\vec{n}_i - \vec{c})^2 E_i / E$, the invariant mass M of the overlapping photons is obtained from the relation $M = E\sqrt{|s - s_\gamma|}$, where s_γ is the average second moment of a single photon shower. This quantity discriminates

between energy clusters deposited by only one photon and by two photons originating from a π^0 decay.

The energy calibration of the electromagnetic calorimeter (NaI crystals, photomultipliers and electronics) uses Bhabha events. Two corrections are applied for single photon showers according to Monte Carlo calculations: 2% for lateral and longitudinal shower leakage and up to 2% for non-central hits in the crystal with the highest energy. An empirical correction for non-linearity is 5% for 100 MeV photons and smaller at higher energies [6]. For merged π^0 's a correction of 6% to the energy measured in the connected region is needed to account for shower leakage according to Monte Carlo studies. From these studies we conclude that our energy scale has a systematic error of 2%. Two different checks of this procedure for energy calibration have been made using our data. From events $\gamma\gamma \rightarrow f_2 \rightarrow \pi^0\pi^0$ with one merged and one unmerged π^0 we find $M_{f_2} = (1271 \pm 5) \text{ MeV}/c^2$ (statistical error only). The reconstructed masses for unmerged and merged π^0 's are $(135.0 \pm 2.1) \text{ MeV}/c^2$ and $(130.2 \pm 2.8) \text{ MeV}/c^2$, respectively.

4 Event selection

The data used in this analysis correspond to an integrated luminosity of 257 pb^{-1} and were collected between 1982 and 1986. The events are required to satisfy the following selection criteria:

- The energy deposited in the main ball must be less than 5000 MeV. This cut is useful in rejecting e^+e^- annihilation events.
- The events must have exactly five connected regions, each of them with an energy $E > 20 \text{ MeV}$, at least one with $E > 500 \text{ MeV}$ (merged π^0 candidate).
- The direction of each shower has to satisfy the angular cut $|\cos\theta| < 0.85$, where θ is the angle between the shower direction and the beam direction.
- The lateral energy distribution of each photon candidate must be consistent with that expected for a single electromagnetically showering particle. This condition is not imposed on the lateral energy distribution of the merged π^0 candidates.
- At most one charged track (detected by the tube chambers) which is correlated with an energy cluster is admitted since the probability for conversion of at least one out of six photons is about 20%.
- The squared transverse momentum sum $|\sum \vec{p}_t|^2$ is required to be less than $15000 \text{ MeV}^2/c^2$. (Events failing this cut have been kept to study the distribution of this quantity).

The data sample after these selection cuts shows a clear π^0 signal. For events with at least one pair of separated photons with an invariant mass in the range from $105 \text{ MeV}/c^2$ to $165 \text{ MeV}/c^2$, a scatter plot of the invariant mass of the remaining two separated photons versus the mass of the two overlapping photons is shown in Fig. 1a. A cluster for $\pi^0\pi^0$ is observed. For invariant masses of the two separated photons from $105 \text{ MeV}/c^2$ to $165 \text{ MeV}/c^2$ and from $80 \text{ MeV}/c^2$ to $180 \text{ MeV}/c^2$ for the two overlapping photons, the invariant mass of the two remaining photons is plotted in Fig. 1b. The widths of the observed signals are consistent with our expected π^0 mass resolutions. Both distributions shown in Fig. 1 clearly present evidence for the observation of $\pi^0\pi^0\pi^0$ events. When these three cuts are imposed simultaneously the resulting final sample consists of 69 events. Only one event is ambiguous with two combinations of isolated photons satisfying the cuts defined above.

The four-momenta of the three π^0 's were used to calculate the invariant mass of the final state. The histogram in Fig. 2a shows this $\pi^0\pi^0\pi^0$ invariant mass distribution. A clear enhancement around $1750 \text{ MeV}/c^2$ is visible. The transverse momentum distribution peaks at small values as is expected for the two-photon production mechanism (see Fig. 3). The invariant mass distribution of the $\pi^0\pi^0$ subsystem is shown in Fig. 4. We observe, above a combinatorial background, an enhancement around $1250 \text{ MeV}/c^2$. This suggests that we observe π_2^- production, followed by the decay into $\pi^0 f_2(1270)$. The π_2 has $J^{PC} = 2^{-+}$ and is thus expected to be produced in quasi-real $\gamma\gamma$ scattering. Consistency of the angular distributions and the mass and width of the observed signal with those expected for the π_2 are discussed in sections 7 and 8.

5 Detection efficiency

To ensure that the enhancement in the $\pi^0\pi^0\pi^0$ invariant mass distribution does not come from phase space production and to simulate π_2 resonance production and decay, two Monte Carlo event generators were used. Both Monte Carlo data samples were passed through a complete detector simulation.

The first Monte Carlo program (MC1) generated $\gamma\gamma \rightarrow \pi^0\pi^0\pi^0$ events with an energy independent cross section and a decay according to phase space. The $\pi^0\pi^0\pi^0$ invariant mass distribution obtained from MC1 generated events does not reproduce the peak in the data (see Fig. 2a). Also the experimental $\pi^0\pi^0$ invariant mass distribution is not described correctly by MC1 (see Fig. 4).

The second Monte Carlo generator (MC2) is based on a covariant matrix element for the decay chain in (1). The formation of a resonant state with spin-parity 2^- in the collision of two quasi-real photons is described [7] by only one amplitude, which has total helicity 0. Since the final state consists of three indistinguishable pions, the full amplitude must be symmetrized, i.e. expressed in terms of a coherent sum of three amplitudes corresponding to

the three different combinations of π° 's leading to the $\pi^{\circ} f_2(1270)$ final state. The squared matrix element $|\mathcal{M}|^2$ describing the process $\gamma\gamma \rightarrow \pi_2 \rightarrow \pi^{\circ} f_2 \rightarrow \pi^{\circ} \pi^{\circ} \pi^{\circ}$ may be written as:^{*}

$$|\mathcal{M}|^2 = \sigma(\gamma\gamma \rightarrow \pi_2) \cdot BR \cdot M_{\pi_2}^{-1} \cdot |D(1,2) \mathcal{A}(1,2) + D(1,3) \mathcal{A}(1,3) + D(2,3) \mathcal{A}(2,3)|^2, \quad (2)$$

where BR denotes the product decay branching ratio

$$BR = BR(\pi_2 \rightarrow \pi^{\circ} f_2) \cdot BR(f_2 \rightarrow \pi^{\circ} \pi^{\circ})$$

and M_{π_2} is the π_2 mass; $D(i, k)$ and $\mathcal{A}(i, k)$ are defined in (7) and (8) below. The Breit-Wigner cross section for π_2 production is given by [8]

$$\sigma(\gamma\gamma \rightarrow \pi_2) = 8\pi(2J_{\pi_2} + 1) \left(\frac{M_{\pi_2}}{W_{\gamma\gamma}} \right)^2 \frac{\Gamma_{\pi_2}^{\gamma\gamma}(W_{\gamma\gamma}) \cdot \Gamma_{\pi_2}^{tot}(W_{\gamma\gamma})}{(W_{\gamma\gamma}^2 - M_{\pi_2}^2)^2 + (M_{\pi_2} \cdot \Gamma_{\pi_2}^{tot}(W_{\gamma\gamma}))^2}. \quad (3)$$

Here the widths are mass dependent. The total width is given by

$$\Gamma_{\pi_2}^{tot}(W_{\gamma\gamma}) = \Gamma_{\pi_2}^{tot}(M_{\pi_2}) \frac{M_{\pi_2}}{W_{\gamma\gamma}} \left(\frac{q^*}{q_0^*} \right)^{2L+1} \frac{R_L(q_0^* r)}{R_L(q^* r)}, \quad (4)$$

where $\Gamma_{\pi_2}^{tot}(M_{\pi_2})$ is the nominal total width, $q^*(W_{\gamma\gamma})$ is the $f_2(1270)$ momentum in the $\gamma\gamma$ center-of-mass system and $q_0^* = q^*(M_{\pi_2})$. L is the orbital angular momentum between the $f_2(1270)$ and the π° in the final state: it is $L = 0$ in the case of $\pi_2 \rightarrow \pi^{\circ} f_2(1270)$ [9]. The R_L are Blatt-Weisskopf damping factors [10]. Note that $R_0 \equiv 1$ holds.

The decay width of the π_2 to two photons depends [8] on $W_{\gamma\gamma}$:

$$\Gamma_{\pi_2}^{\gamma\gamma}(W_{\gamma\gamma}) = \left(\frac{W_{\gamma\gamma}}{M_{\pi_2}} \right)^4 \Gamma_{\pi_2}^{\gamma\gamma}(M_{\pi_2}). \quad (5)$$

The nominal width is parametrized as [8]

$$\Gamma_{\pi_2}^{\gamma\gamma}(M_{\pi_2}) = \frac{M_{\pi_2}^3}{120\pi} F^2(q_1^2 = 0, q_2^2 = 0), \quad (6)$$

where $F(0, 0)$ is the helicity form factor (the $\gamma\gamma$ - π_2 coupling constant) which does not depend on either the $\gamma\gamma$ invariant mass or the resonance mass. It can therefore be used for comparison of resonances.

The $D(i, k)$ symbol in (2) denotes the decay amplitude of $\pi_2 \rightarrow \pi^{\circ} f_2, f_2 \rightarrow \pi_i^{\circ} \pi_k^{\circ}$ with the f_2 propagator separated out. $D(i, k)$ can be interpreted as the combined angular distribution of the π_2 and the f_2 decays. All quantities here and in the following are calculated in the rest frame of the $\gamma\gamma$ system with the z -axis oriented along the beam axis. These amplitudes

^{*}In this notation the integral of $|\mathcal{M}|^2$ over the $\pi^{\circ} \pi^{\circ} \pi^{\circ}$ phase-space volume is equal to $\sigma(\gamma\gamma \rightarrow \pi_2) \cdot BR$.

were parametrized in a covariant way as given in [8]. The helicity-0 amplitude describing the $\pi_2 \rightarrow \pi^0 f_2$ decay takes the form

$$D(1,2) = \frac{1}{\sqrt{6}} \left\{ \vec{k}_-^2 (3 \cos^2 \theta_- - 1) + \vec{k}_+^2 (3 \cos^2 \theta_+ - 1) \frac{E_-^2}{(E_+ - m_{12})^2} - \frac{2E_-}{(E_+ - m_{12})} (3k_-^z k_+^z - \vec{k}_- \cdot \vec{k}_+) \right\} \quad (7)$$

with (E_1, \vec{k}_1) and (E_2, \vec{k}_2) being the four-momenta of the π^0 's from the f_2 decay, $\vec{k}_\pm = \vec{k}_1 \pm \vec{k}_2$, $E_\pm = E_1 \pm E_2$, m_{12} the $\pi_1 \pi_2$ invariant mass, and θ_\pm the polar angle of \vec{k}_\pm with respect to the beam axis.

The amplitudes $\mathcal{A}(i, k)$ in the symmetrized matrix element (2) are proportional to Breit-Wigner propagators for the $f_2(1270)$, for instance

$$\mathcal{A}(1,2) \propto \frac{1}{(m_{12}^2 - M_{f_2}^2) - i \Gamma_{f_2}^{tot} M_{f_2}}. \quad (8)$$

The width $\Gamma_{f_2}^{tot}$ depends on the $\pi^0 \pi^0$ invariant mass m_{12} as given in (4), substituting m_{12} for $W_{\gamma\gamma}$ and using $R_2 = 9 + 3(q^* r)^2 + (q^* r)^4$ with $r = 1$ fm.

The detection efficiency was determined on the basis of the MC2 simulation. It is displayed in Fig. 2b. The efficiency is rather small ($\approx 1\%$). Compared to the case of isotropic π_2 decay it is smaller by almost a factor two mainly due to the angular distribution which causes the π^0 's from the f_2 decay to be peaked forward (see discussion below).

6 Background estimate

Possible sources of background under the π_2 signal are non-resonant $\gamma\gamma \rightarrow \pi^0 \pi^0 \pi^0$ production and non-exclusive final states, $\pi^0 \pi^0 \pi^0 + X$, produced either in two-photon scattering or beam-gas reactions. The first channel would have a peaked $|\sum \vec{p}_i|^2$ distribution similar to the data (Fig. 3), whereas this distribution for the second and the third channel is expected to be flat. Comparison of the experimental $|\sum \vec{p}_i|^2$ distribution for events having $M(\pi^0 \pi^0 \pi^0) > 1450$ MeV/c² with that obtained from MC2 (see Fig. 3) shows close agreement of the two, suggesting a rather small non-exclusive background contribution in the resonance region.

The $|\sum \vec{p}_i|^2$ distribution for events below 1450 MeV/c² is flat, indicating that those events are non-exclusive background. After our $|\sum \vec{p}_i|^2$ cut ten such events remain (Fig. 2a). The amount of background under the signal was then determined by a fit (see section 8), which found 4.8 background events in the resonance region, which contains 59 events total. The background resulting from this fit is shown in Fig. 2a.

7 Angular distributions

To check the consistency of our signal with the known spin and parity of the π_2 , decay angular distributions have been studied for the events with $M(\pi^0\pi^0\pi^0) > 1450 \text{ MeV}/c^2$. As stated above, a 2^- resonance produced in quasi-real two-photon collisions has helicity 0 relative to the momentum vector of the two-photon system, which approximately coincides with the beam direction. Since the relative orbital angular momentum in the decay $\pi_2 \rightarrow \pi^0 f_2$ is $L = 0$ [9], the projection of the f_2 spin on an axis parallel to the beam must be identical to that of the π_2 . This determines both angular decay distributions: the distribution $\pi_2 \rightarrow \pi^0 f_2$ has to be isotropic, whereas the distribution $f_2 \rightarrow \pi^0\pi^0$ is expressed in terms of spherical harmonics as $|Y_2^0(\theta)|^2$. Here θ is the polar angle of the f_2 decay pions evaluated in the f_2 rest frame with the z -axis oriented along the beam direction.

A kinematical analysis shows that the most energetic (“fast”) π^0 nearly always originates from the f_2 decay. Unfortunately it is not possible to determine unambiguously which of the two remaining π^0 's originates from the f_2 decay. However, one can investigate the $|\cos\theta^*|$ distribution of the fast π^0 in the $\gamma\gamma$ rest frame. The distribution of the data is presented together with those of the two Monte Carlo simulations in Fig. 5a. We find reasonable agreement between the data and the MC2 angular distribution ($\chi^2 = 5.1$ for 4 d.o.f.) whereas the data and the MC1 distributions disagree ($\chi^2 = 31.6$ for 4 d.o.f.). This shows that the experimental angular distribution agrees with the one expected from the π_2 decay via a $\pi^0 f_2$ intermediate state.

The spin-parity assignment of the resonance may be further tested by analyzing the angular distribution of the two low energy pions. This distribution should be flatter as it contains also the isotropic distribution of the direct π^0 from the $\pi_2 \rightarrow \pi^0 f_2$. It is plotted together with that obtained from MC2 in Fig. 5b. The two distributions are in good agreement ($\chi^2 = 4.2$ for 4 d.o.f.). The MC1 distribution does not agree ($\chi^2 = 14.5$ for 4 d.o.f.).

Another test of the spin-parity hypothesis is performed by investigating the polar angular distribution of the normal to the decay plane of the $\pi^0\pi^0\pi^0$ system in its rest frame (all three π^0 momenta are coplanar). In Fig. 6 the data are compared to the MC1 and MC2 distributions. The agreement is good ($\chi^2 = 2.3$ for 4 d.o.f.) for MC2 whereas MC1 does not fit the data ($\chi^2 = 13.1$ for 4 d.o.f.).

These studies of angular distributions support the hypothesis that we observe the decay chain $\pi_2 \rightarrow \pi^0 f_2 \rightarrow \pi^0\pi^0\pi^0$.

8 Resonance parameters

In order to determine the π_2 resonance parameters the Breit-Wigner shape in (3), convoluted with resolution (42 MeV) and corrected for flux and efficiency, was fitted to the $M(\pi^0\pi^0\pi^0)$

distribution of Fig. 2a. The efficiency was calculated by MC2, which assumes the reaction chain (1). An unbinned maximum likelihood method was used. In addition to the Breit-Wigner shape, a linear background was assumed. Its amplitude was fixed to account for the ten events below $1450 \text{ MeV}/c^2$ and its slope was allowed to vary. The other parameters to the fit are the mass M_{π_2} , the total width $\Gamma_{\pi_2}^{tot}$ and for the $\gamma\gamma$ partial width $\Gamma_{\pi_2}^{\gamma\gamma} \cdot BR(\pi_2 \rightarrow \pi^0\pi^0\pi^0)$. The curve resulting from the fit is shown in Fig. 2a. The values of the parameters obtained in the fit are (the first error is statistical, the second systematic)

$$\begin{aligned} M_{\pi_2} &= (1742 \pm 31 \pm 49) \text{ MeV}/c^2 \\ \Gamma_{\pi_2}^{tot} &= (236 \pm 49 \pm 36) \text{ MeV} \\ \Gamma_{\pi_2}^{\gamma\gamma} \cdot BR &= (251 \pm 40 \pm 35) \text{ eV}. \end{aligned}$$

The systematic errors are shown in Table 1. The systematic uncertainty in the detection efficiency contains, besides Monte Carlo statistics, the error on the chamber inefficiency. The selection cuts on the π^0 mass (merged and unmerged), on the solid angle and on the $|\sum \vec{p}_t|^2$ have been varied. The contribution to the systematic error from background subtraction was taken as the difference between the fit parameters obtained above and those obtained under the extreme assumption of no background under the resonance. The individual contributions have been combined in quadrature.

In order to obtain the cross section, the background as given by the fit is first subtracted. Then the data are corrected for the $\gamma\gamma$ -flux of two transverse photons and for the efficiency. The resulting cross section for the reaction $\gamma\gamma \rightarrow \pi_2 \rightarrow \pi^0 f_2 \rightarrow \pi^0\pi^0\pi^0$ in the invariant mass range from $1450 \text{ MeV}/c^2$ to $2500 \text{ MeV}/c^2$ is displayed in Fig. 7. The intermediate state $\pi^0 f_2$ has to be specified since the efficiency is calculated under this assumption. The cross section curve obtained from the fit described above is also shown in Fig. 7.

The main decay mode for the π_2 into three pions is via the $\pi^0 f_2(1270)$ intermediate state [1]. One experiment [9] has reported that the π_2 also decays into a $\pi(\pi\pi)_{S\text{-wave}}$. Including this result, the Particle Data Group [1] has found the following values for the branching ratios:

$$\begin{aligned} BR(\pi_2 \rightarrow \pi^0 f_2 \rightarrow \pi^0\pi^0\pi^0) &= BR(\pi_2 \rightarrow \pi^0 f_2) \cdot BR(f_2 \rightarrow \pi\pi) \cdot \frac{1}{3} \\ &= (53 \pm 5) \% \cdot (86_{-1}^{+2}) \% \cdot \frac{1}{3} = (15.2 \pm 1.5) \% . \\ BR(\pi_2 \rightarrow \pi^0(\pi^0\pi^0)_{S\text{-wave}}) &= BR(\pi_2 \rightarrow \pi(\pi\pi)_{S\text{-wave}}) \cdot \frac{1}{3} = (9 \pm 5) \% \cdot \frac{1}{3} . \end{aligned}$$

Using these branching ratios, the topological branching ratio is

$$BR \equiv BR(\pi_2 \rightarrow \pi^0\pi^0\pi^0) = (18.2 \pm 2.3) \% .$$

The contribution of the $\pi^0(\pi^0\pi^0)_{S\text{-wave}}$ mode should manifest itself in the invariant mass distribution of the $\pi^0\pi^0$ subsystem. Our data on the $M_{\pi^0\pi^0}$ distribution (Fig. 4) show an

enhancement at the f_2 mass above a combinatorial background and are in good agreement with MC2, while disagreeing with MC1. With our limited statistics a small contribution from the $(\pi^0\pi^0)_{S\text{-wave}}$ in π_2 decays cannot be measured.

To calculate $\Gamma_{\pi_2}^{\gamma\gamma}$ we assume an S-wave contribution as given above. The detection efficiency for the $\pi^0(\pi^0\pi^0)_{S\text{-wave}}$ decay has been determined from Monte Carlo simulation and is somewhat smaller than for the $\pi^0 f_2(1270)$ decay, as may be seen in Fig. 2b. The difference in efficiency is taken into account in calculating the partial width. We find

$$\Gamma_{\pi_2}^{\gamma\gamma} = (1.45 \pm 0.23 \pm 0.28) \text{ keV}.$$

Our results on M_{π_2} and $\Gamma_{\pi_2}^{tot}$ are consistent with the values quoted by the Particle Data Group [1]. It should be noted that the mean value of $M_{\pi_2} = (1670 \pm 20) \text{ MeV}/c^2$ [1] does not take into account the result from a two-resonance fit [9], which yielded $M_{\pi_2} = (1710 \pm 15) \text{ MeV}/c^2$. Also the experiment which observed the $\pi_2^- \rightarrow \mu^+ \mu^- \pi^-$ channel [11] found a similar value, $(1710 \pm 20) \text{ MeV}/c^2$. In this channel a mass shift due to final state interactions should be minimal, as in the $\gamma\gamma$ formation of the π_2 .

Our result on $\Gamma_{\pi_2}^{\gamma\gamma}$ agrees within the large errors of both experiments with the recent analysis of the CELLO Collaboration [3] which obtained $\Gamma_{\pi_2}^{\gamma\gamma} = (0.8 \pm 0.3 \pm 0.12) \text{ keV}$ observing the decay channel $\pi_2 \rightarrow \pi^+ \pi^- \pi^0$. Two intermediate states can contribute to this final state: $\pi^0 f_2(1270)$ and $\pi\rho$ (the latter is forbidden in the $\pi^0\pi^0\pi^0$ final state). The CELLO result given above assumes constructive interference of the two intermediate states. If they assume incoherence they get $\Gamma_{\pi_2}^{\gamma\gamma} = (1.3 \pm 0.3 \pm 0.2) \text{ keV}$, in better agreement with our data.

The value of $\Gamma_{\pi_2}^{\gamma\gamma}$ can be converted into the corresponding coupling constant F . Using (6) and our value of M_{π_2} one obtains

$$F(\pi_2) = (10.2 \pm 1.4) \cdot 10^{-6} \text{ MeV}^{-1}.$$

In this quantity mass dependent factors like phase space have been separated out. Then the coupling constant is, apart from constant factors, equal to the hadronic matrix element. Its value can be compared more readily to that of other mesons to gain a feeling about the hadronic wave functions and especially their flavor dependence. The coupling constant for the π^0 meson is[†] $F(\pi^0) = (24.8 \pm 0.3) \cdot 10^{-6} \text{ MeV}^{-1}$. But one has to keep in mind that for the π^0 meson ($L = 0$) the coupling constant F depends on the wave function at the origin, $\psi(0)$, whereas for the π_2 meson ($L = 2$) it depends on $\psi''(0)$. Nonetheless, such similar values of F argue against an exotic nature of the π_2 .

9 Conclusion

The first observation of $\gamma\gamma$ production of the neutral member of the π_2 isotriplet in the $\pi^0\pi^0\pi^0$ final state has been reported. The measurement of the two-photon partial width and new

[†]Note that for pseudoscalar mesons the factor 120 in Eq. (6) must be changed to 64.

values for the mass and the total width of the π_2 are presented. The π_2 is the first resonant state with $J^{PC} = 2^{-+}$ to be observed in two-photon interactions. The values of $\Gamma_{\pi_2}^{\gamma\gamma}$ and the form factor F are comparable to those obtained for mesons in other nonets. This suggests that the π_2 is a conventional $q\bar{q}$ meson.

Acknowledgements

We would like to thank the DESY and SLAC directorates for their support. This experiment would not have been possible without the dedication of the DORIS machine group as well as the experimental support groups at DESY. The visiting groups thank the DESY laboratory for the hospitality extended to them. Z.J., B.N., B.Muryn, and G.N. thank DESY for financial support. E.D.B., R.H., and K.S. have benefitted from financial support from the Humboldt Foundation. K. Königsmann acknowledges support from a Heisenberg fellowship. We thank M. Poppe and J. Olsson for valuable discussions. B.Muryn thanks U. Karshon for the hospitality extended to him during the VIII International Workshop on Photon-Photon Collisions in Shresh.

References

- [1] Particle Data Group, G.P. Yost *et al.*: *Review of Particle Properties*, Phys. Lett. B 204 (1988) 1.
- [2] B. Muryn, in: VIIIth International Workshop on Photon-Photon Collisions, Shresh/Israel, 24-28 April 1988, U. Karshon (editor), World Scientific (1988), p.102.
- [3] H.-J. Behrend *et al.* (CELLO Collaboration): DESY 89-177; Z. Phys. C, to be published.
- [4] D.A. Williams *et al.*: Phys. Rev. D 38 (1988) 1365;
K. Wachs *et al.*: Z. Phys. C 42 (1989) 33.
- [5] P. Schmitt *et al.*: Z. Phys. C 40 (1986) 199.
- [6] D. Gelphman: Ph.D. Thesis, Stanford University, SLAC-286 (1985), unpublished.
- [7] L.D. Landau: Sov. Phys. Doklady 60 (1948) 207;
C.N. Yang: Phys. Rev. 77 (1950) 242.
- [8] V.M. Budnev *et al.*: Phys. Rep. 15 (1975) 181;
M. Poppe: Int. J. Mod. Phys. A 1 (1986) 545, and private communication.
- [9] C. Daum *et al.* (ACCMOR Collaboration): Nucl. Phys. B 182 (1981) 269.
- [10] J.M. Blatt, V. Weisskopf: *Theoretical Nuclear Physics*, New York (1952).
- [11] Y.M. Antipov *et al.*: Europhys. Lett. 4 (1987) 403.

Table

Source	M	Γ^{tot}	$\Gamma_{\gamma\gamma} \cdot BR$	$\Gamma_{\gamma\gamma}$
Luminosity	—	—	$\pm 3\%$	$\pm 3\%$
Absolute energy calibration	$\pm 2\%$	—	$\pm 3\%$	$\pm 3\%$
Detection efficiency	$\pm 1.5\%$	$\pm 3\%$	$\pm 10\%$	$\pm 10\%$
Background subtraction and cut variation	$\pm 1.3\%$	$\pm 15\%$	$\pm 8\%$	$\pm 8\%$
Branching ratio	—	—	—	$\pm 13\%$
Combined	$\pm 2.8\%$ $\pm 49 \text{ MeV}$	$\pm 15\%$ $\pm 36 \text{ MeV}$	$\pm 14\%$ $\pm 35 \text{ eV}$	$\pm 19\%$ $\pm 0.28 \text{ keV}$

Table 1: Systematic errors: contributions to the results on Mass M_{π_2} , total width $\Gamma_{\pi_2}^{tot}$ and $\gamma\gamma$ partial width $\Gamma_{\pi_2}^{\gamma\gamma}$, with and without the branching ratio BR .

Figure Captions

1. The invariant mass distributions of two photons.
 - a) Scatter plot of the invariant mass of two separated photons versus the mass of two overlapping photons (the remaining two separated photons are in the mass range from $105 \text{ MeV}/c^2$ to $165 \text{ MeV}/c^2$). The cut window is displayed.
 - b) The invariant mass of two separated photons. The invariant mass of the remaining two separated photons and the mass of the two overlapping photons are required to be in the mass range from $105 \text{ MeV}/c^2$ to $165 \text{ MeV}/c^2$ and from $80 \text{ MeV}/c^2$ to $180 \text{ MeV}/c^2$, respectively. The cuts are indicated by arrows.
2. a) The observed invariant mass distribution of the $\pi^0\pi^0\pi^0$ events (histogram), the expectation from MC1 (dotted line), the result of the fit (solid line), and the background contribution to the fit (dashed line).
 - b) The detection efficiencies determined from MC1 (dotted line), MC2 (solid line) and the Monte Carlo for the $\pi_2 \rightarrow \pi(\pi\pi)_{S\text{-wave}}$ decay (dashed line). For details see text.
3. The $|\sum \vec{p}_i|^2$ distribution of $\pi^0\pi^0\pi^0$ events with one merged and two unmerged π^0 's and having $M(\pi^0\pi^0\pi^0) > 1450 \text{ MeV}/c^2$. Dots with error bars are the data points whereas the histogram represents the MC2 prediction. The arrow indicates the cut.
4. The invariant mass distribution of the $\pi^0\pi^0$ subsystems (3 entries/event) for events with $M(\pi^0\pi^0\pi^0) > 1450 \text{ MeV}/c^2$. Dots with error bars represent the data. The solid histogram is the MC2 prediction; the dotted histogram is the MC1 prediction.
5. Polar angular distributions of the π^0 's in the rest frame of the $\gamma\gamma$ system for events with $M(\pi^0\pi^0\pi^0) > 1450 \text{ MeV}/c^2$. The data are not corrected for detection efficiency. The distributions are normalized to unit area.
 - a) Angular distributions of the fast π^0 (see text). The points with error bars are the experimental data. The solid histogram is the MC2 result, while the dotted line represents the MC1 prediction.
 - b) Angular distribution of the two low energy pions (2 entries per event). Notation as in (a).
6. Polar angular distribution of the normal to the decay plane in the $\gamma\gamma$ rest frame for events with $M(\pi^0\pi^0\pi^0) > 1450 \text{ MeV}/c^2$. The points with error bars are the experimental data, not corrected for efficiency. The solid histogram is the MC2 result. The dotted line represents MC1. All distributions are normalized to unit area.
7. The cross section $\sigma(\gamma\gamma \rightarrow \pi_2) \cdot BR(\pi_2 \rightarrow \pi^0\pi^0\pi^0)$, measured assuming the decay chain $\pi_2 \rightarrow \pi^0 f_2 \rightarrow \pi^0\pi^0\pi^0$, as a function of the $\gamma\gamma$ center of mass energy $W_{\gamma\gamma}$. The solid curve shows the result of the Breit-Wigner fit to the data of Fig. 2.

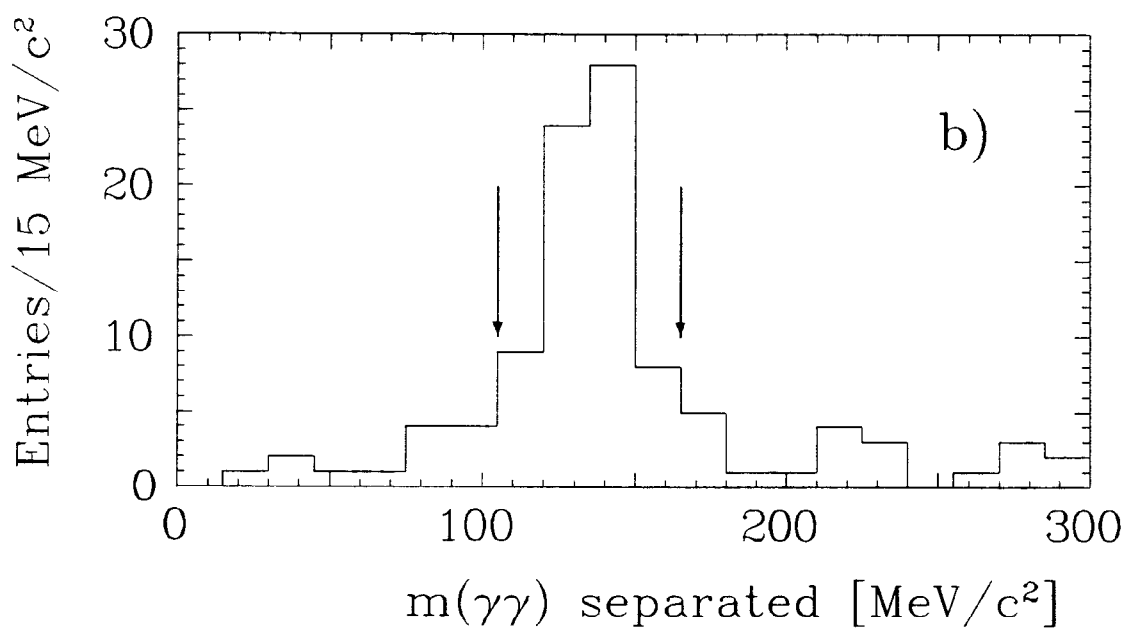
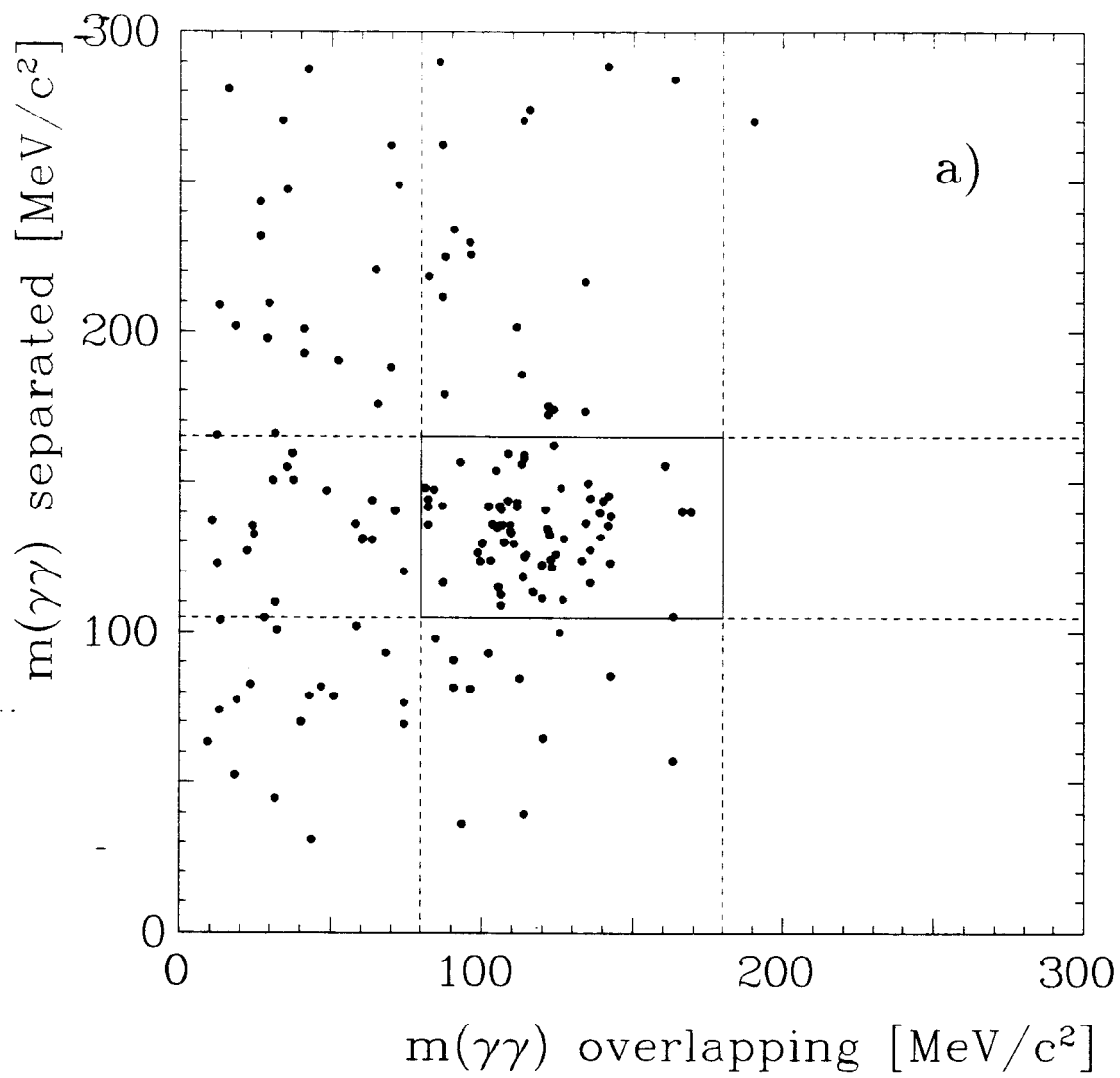


Figure 1

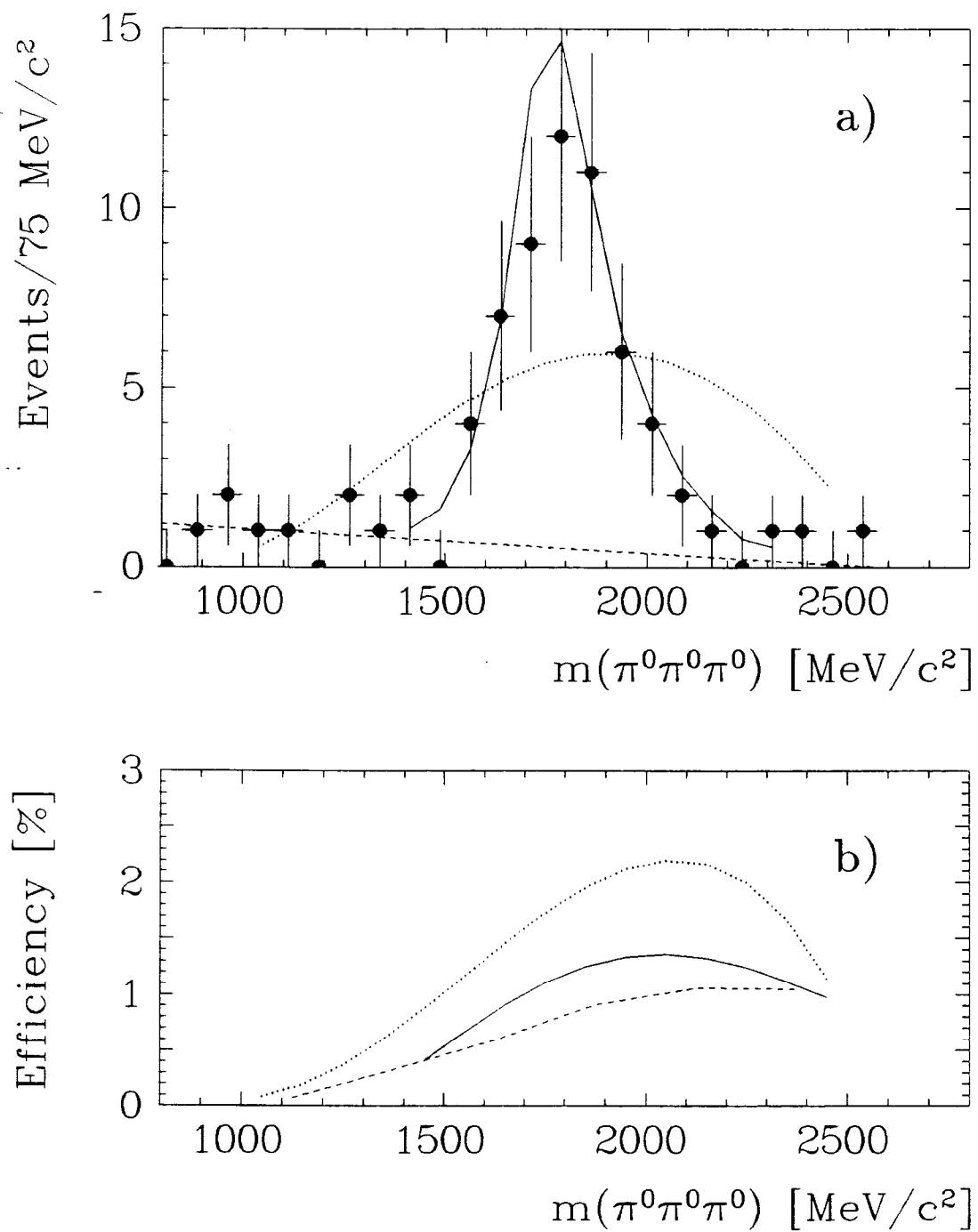


Figure 2

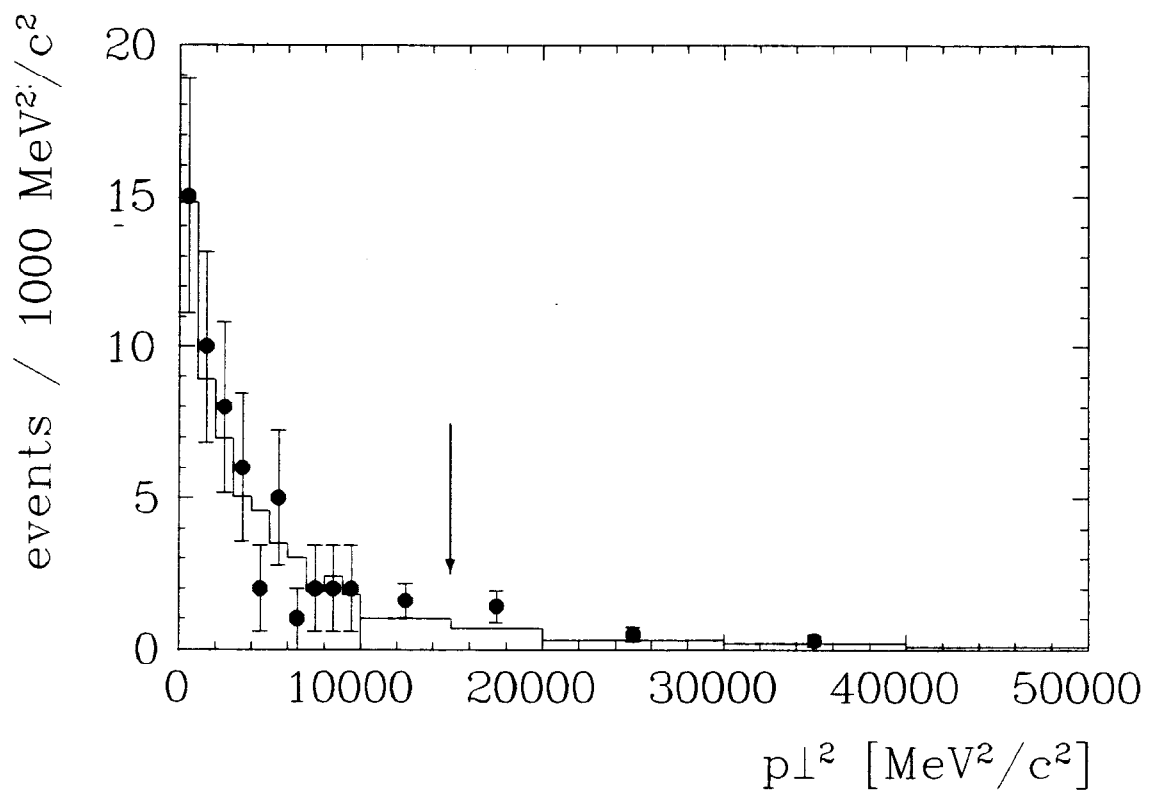


Figure 3

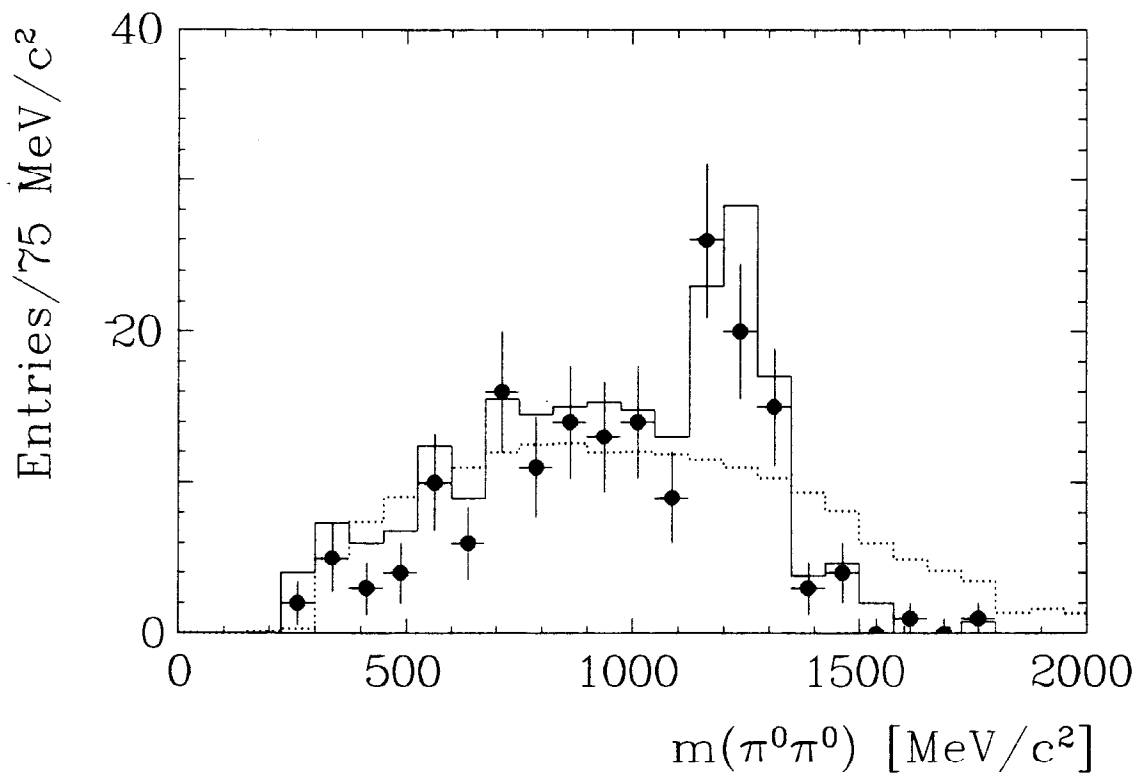


Figure 4

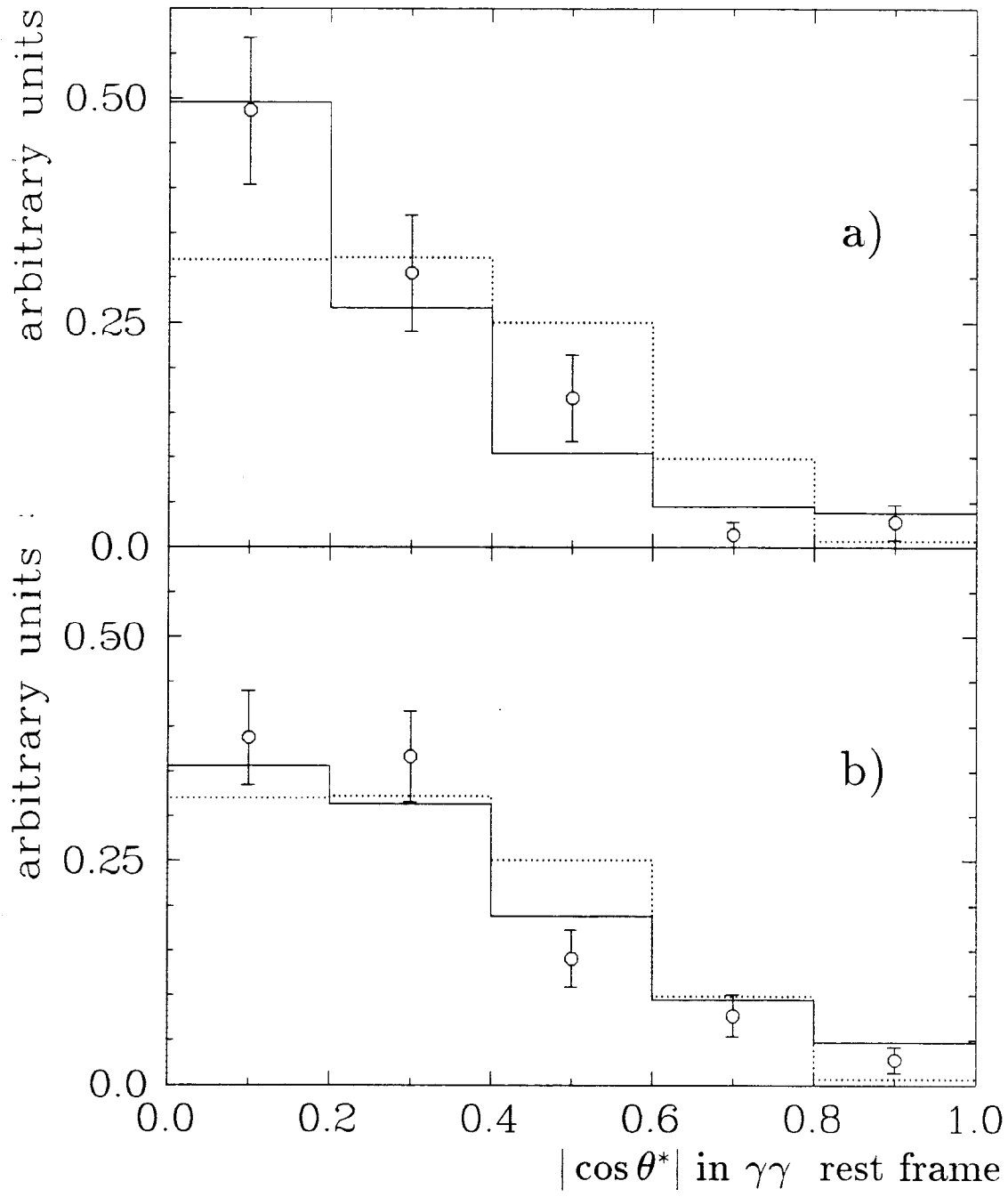


Figure 5

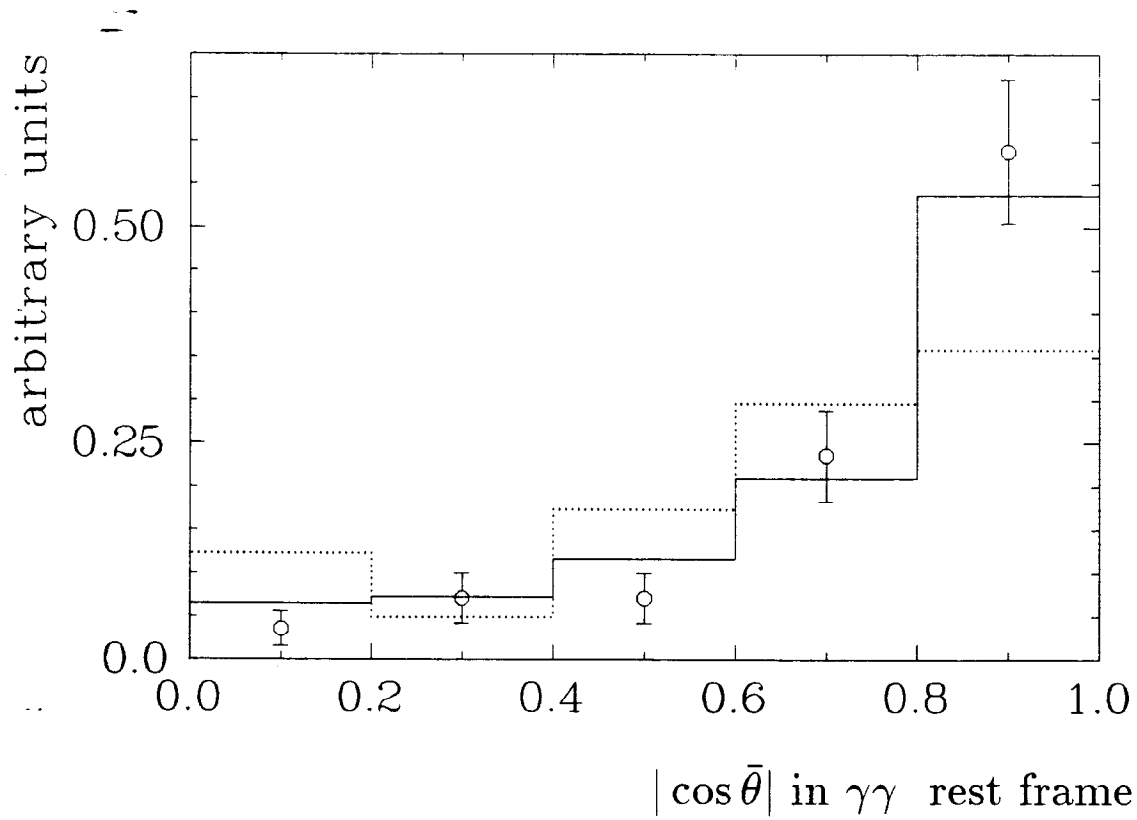


Figure 6

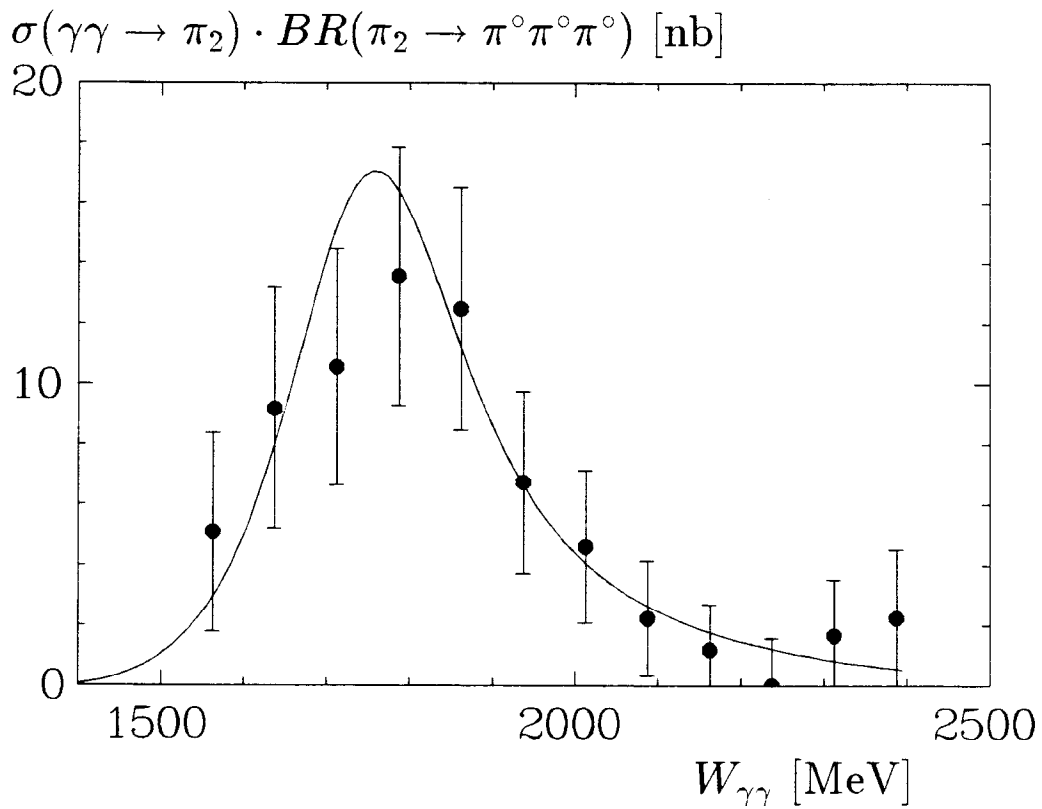


Figure 7